IEEE Access
Multidisciplinary | Rapid Review | Open Access Journal

Received February 26, 2019, accepted March 24, 2019, date of publication March 27, 2019, date of current version April 10, 2019.

Digital Object Identifier 10.1109/ACCESS.2019.2907813

A Novel Infrared Focal Plane Non-Uniformity Correction Method Based on Co-Occurrence Filter and Adaptive Learning Rate

LI LINGXIAO, LI QI, FENG HUAJUN, XU ZHIHAI, AND CHEN YUETING

State Key Laboratory of Modern Optical Instrumentation, Zhejiang University, Hangzhou 310027, China

Corresponding author: Li Qi (liqi@zju.edu.cn)

This work was supported in part by the Yunnan Provincial Department of Education Science Research Fund Project under Grant 2016FC002, and in part by the Science and Technology, Zhejiang University, under Project 2017C01033.

ABSTRACT Non-uniformity commonly exists in the infrared focal plane, which behaves as the fixed pattern noise (FPN) and seriously affects the image quality of the infrared imaging system. This paper proposed a novel scene-based non-uniformity correction method with a new edge-preserve filter and adaptive learning rate. First, using co-occurrence filter as the desired image estimation, the proposed method removed the FPN while preserving the image details. Then, an adaptive learning rate connected with both temporal motion and spatial correlation factor is utilized to decrease the effect of ghosting artifacts. In this way, the proposed method overcomes the shortcomings of the traditional scene-based non-uniformity. Several real infrared image sequences collected in different conditions are used to verify the performance of the proposed method. The experimental results demonstrate that the proposed method has a much better visual effect, making a great balance between the non-uniformity correction and details preservation. Compared with other good NUC methods, this method also has better performance in the aspects of applicability and robustness, which has great application value.

INDEX TERMS Non-uniformity correction, IRFPA, edge-preserve filter, adaptive learning rate, ghosting artifacts, details preservation.

I. INTRODUCTION

Infrared focal plane array (IRFRA) is the core component of infrared imaging systems which is widely used in related technical fields such as industrial, security and remote sensing, etc. However, due to external environment, infrared sensitive components, circuit structure and semiconductor characteristics, the response under the same infrared irradiance varies between the different unit within an IRFPA. This phenomenon will impose the fixed pattern noise (FPN) in the infrared image which is called non-uniformity of IRFPA [1], and the non-uniformity has a serious impact on the sensitivity and the quality of IRFPA imaging system. Therefore, it is necessary to perform non-uniformity correction (NUC) on the acquired infrared image for subsequent target detection and recognition.

The associate editor coordinating the review of this manuscript and approving it for publication was Chaker Larabi.

The NUC methods can be divided into two main categories: (1) the reference-based non-uniformity correction (RBNUC) and (2) the scene-based non-uniformity correction (SBNUC) [4]. RBNUC method mainly contains one-point, two-point and multi-point correction methods [2]–[3]. These methods employ uniform blackbody at different temperatures as reference irradiance sources to calculate the correction parameter, which based on the linear relationship between IRFPA response and temperature. The advantages of these methods are simplicity and low computational complexity. However, periodically calibration is needed due to the temporal drift effect of response, which could interrupt the process and prevent real-time correction of the imaging system. On the other hand, scene-based NUC method is well developed because the correction parameter of SBNUC only depends on the information of the imaging scene, which could reduce the operation complexity and avoid imaging interruption. Besides, the FPN drifted over time could be suppressed automatically during NUC process

with scene moves, therefore the method of SBNUC is an important research direction of infrared non-uniformity correction technology in recent years.

SBNUC methods have been proposed over the years and can be broadly classified into four categories, which are the statistics based method, the temporal filtering based method, the registration based method and the optimal estimation based method [9]. For the statistics based method, Constant Statistics (CS) [5] is the typical way which assumes that the temporal mean and variance of each pixel are identical, and estimate the related correction parameters. However, this method heavily relies on the scene moving and have to spend much time to converge; The Temporal High-Pass filtering (THP) based method [6] sets a high-pass filtering in the temporal domain and the FPN will be removed due to its low-frequency characteristic. However, The THP method will also remove the static object feature and cause serious ghosting artifact. Although some improved methods such as the Space Low-pass and Temporal High-pass (SLTH) algorithm [7] and the Bilateral-Filter-based Temporal High-pass (BFTH) algorithm [8] are trying to overcome this problem, the cut-off frequency of the spatial filter and the temporal filter are difficult to determine, and the ghosting artifact still exists as well; The registration-based method [10]–[11] assumes that different infrared detection units have identical response when observing the same scene position and the difference response is mainly caused by the FPN. However, the accuracy of registration affects the NUC performance seriously, as a result, this method could not correct the imaging scenes with weak infrared radiation or less image detail feature. Besides, the registration-based method is also lack of robustness and adaptability because of ignoring any scaling, rotation or other warping of the image.

Recently more and more researchers are working on the design of the optimal estimation based method of NUC. It usually makes good use of the minimal energy of the image's gradient in some direction and constructs loss function between the output and desired value to constrain the FPN of IRFPA [12]–[17]. One classical method is combined the least mean square (LMS) error estimation and the neural network model, which including NN-NUC [13], BF-NUC [14], TV-NUC [15]–[16] and GF-NUC [17], and etc. These algorithms iteratively calculate the NUC parameters according to the LMS error between the corrected images and their desired images, which are well-known for their low cost of computation and storage resources. However, the main drawbacks of these algorithms are that they would still easily result in ghosting artifact to the moving object and image blurring to static scene, which restrict in practical application.

Considering the drawbacks of the current LMS based methods, especially the ghosting artifact interruption, this paper proposes a novel NUC method of IRFPA based on the combination of an improved edge-preserve filter called co-occurrence filter and the adaptive learning rate related with both the temporal motion and spatial correlation factor. The key idea is that we apply the co-occurrence filter to remove FPN, and an adaptive learning rate is designed to suppress the ghosting artifact. In this way both the NUC result and visual effect could be optimized. Several real infrared sequences are adopted to test its performance, and experimental results indicate that this method can correct the non-uniformity effectively with few FPN residues left. Besides, the correction result scarcely exists ghosting artifact which could be applied into the real-time infrared image system.

The remainder of paper is organized as follows: In Section II, a brief review of the NUC model and typical LMS based method are presented. In Section III, an improved method based on the co-occurrence filter to get desired image is proposed. In Section IV, an adaptive learning rate based on motion guidance and local spatial correlation detection is put forward to suppress the ghost effect. In Section V, the proposed algorithm is applied to several real infrared image sequences, the correction results are discussed in Section VI and finally the conclusion is given in Section VII.

II. RELATED WORK

A. IRFPA AND NUC RESPONSE MODEL

D The response of each detection-element in an IRFPA can be approximated as a linear model, which is widely used and accepted. The linear model can be defined as follows:

$$X_n(i,j) = a_n(i,j) \cdot Y_n(i,j) + b_n(i,j) \tag{1}$$

where n is the frame number, $X_n(i,j)$ is the response of detection unit (i,j), $Y_n(i,j)$ is the real infrared radiation received by IRFPA, $a_n(i,j)$ and $b_n(i,j)$ are the linear model parameters respectively. NUC algorithms aim to acquire the real radiation value $Y_n(i,j)$ by estimating the correction coefficients from the output response $X_n(i,j)$, that is:

$$Y_n(i,j) = G_n(i,j) \cdot X_n(i,j) + O_n(i,j) \tag{2}$$

$G_n(i,j) = 1/a_n(i,j)$ and $O_n(i,j) = -b_n(i,j)/a_n(i,j)$ are the NUC gain and offset correction coefficients respectively. Essentially, the core process of NUC is to calculate the proper parameters of gain and offset.

B. LMS BASED METHODS OF NUC

LMS based method is derived from Scribner's algorithm [11] which is essentially a neural network, every infrared pixel is treated as a neuron. Through a hidden layer, the pixel can be connected to surround pixels. The sketch map of the neural network model is indicated in Fig.1.

Moreover, Scribner's algorithm first defines the desired image which is expected to be the reference image and free from fixed pattern noise. However, the reference images, or the ideal images are unknown in the real infrared sequences. The general approach is to estimate the desired image from the observed infrared image sequences by filtering the highfrequency FPN by the spatial low pass filter, such as the mean filter, Gaussian filter, and bilateral filter, and etc. Then, the NUC parameters of each pixel are adaptively adjusted by the fast descent method so that the NUC

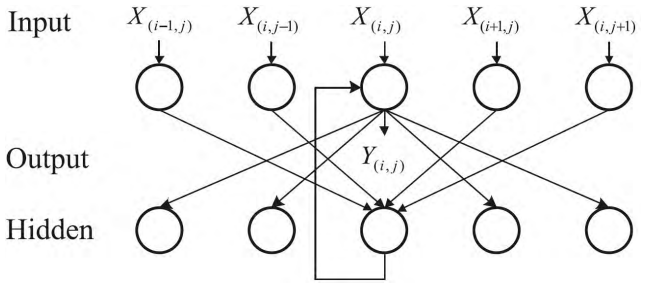

FIGURE 1. Sketch map of the neural network model of NUC.

images are equivalent or approximate to the desired images. The error image between the corrected image and desired image can be defined by:

$$E_n(i,j) = Y_n(i,j) - D_n(i,j) \tag{3}$$

where $E_n(i,j)$ is the error image, $Y_n(i,j)$ is the corrected image, $D_n(i,j)$ is the desired image. For example, in the traditional NN-NUC method, the desired image $D_n(i,j)$ is estimated by the mean value of the nearest 4 neighbor pixels.

The LMS based algorithm seeks to enforce $Y_n(i,j)$ close to $D_n(i,j)$, thus the steepest descent algorithm is applied to minimize the instantaneous square error $E_n^2(i,j)$. Combining Eq. (2) and (3), the error function F is given by:

$$F(G,O) = E^2 = (G \cdot X + O - D)^2 \tag{4}$$

The iteration direction is given by the derivative of G and O respectively, that is:

$$\begin{aligned} F_G &= \frac{\partial F}{\partial G} = 2X \cdot (G \cdot X + O - D) = 2X \cdot (Y - D) \\ F_O &= \frac{\partial F}{\partial O} = 2(G \cdot X + O - D) = 2(Y - D) \end{aligned} \tag{5}$$

In the steepest descent algorithm, the parameters are updated recursively with a step size of each respective error gradient. Thus the inter-frame connection of input image sequences could be indicated as follows:

$$\begin{aligned} G_{n+1}(i,j) &= G_n(i,j) - 2\lambda_n(i,j)X_n(i,j)\,(Y_n(i,j) - D_n(i,j)) \\ O_{n+1}(i,j) &= O_n(i,j) - 2\lambda_n(i,j)\,(Y_n(i,j) - D_n(i,j)) \end{aligned} \tag{6}$$

where $\lambda_n(i,j)$ is the iteration learning rate which determine the convergence speed of the algorithm. For each incoming frame, desired image is first calculated, and the NUC parameters are updated accordingly. Then the new parameters are used to correct the next frame. Thus the NUC parameters in one frame are obtained by previous frames, repeat this process and finally the NUC parameters tend to convergence.

However, during the NUC process the ghosting artifacts are always existing because the accumulation of residuals caused by the error of desired and ideal image. As the algorithm iteratively updates the NUC parameters according to the desired images with residuals, a fraction of parameters corresponding to edge area of images are easily interfered by the residuals. Therefore, the residuals of the updated NUC parameters will keep the old scene still visibly superposed on the new corrected scene, and hence generates ghosting artifacts. To avoid them, the most common method is derived from Hardie's that added the temporal motion detection criterion which is connected with learning rate of the NUC parameters in Scribner's algorithm [18]. The learning rate would be gated when the temporal motion level is small. In other words, the principle of the NUC parameters updating is no motion, no update [19]. Specifically, the learning rate is calculated according to the following rules:

$$\lambda_n(i,j) = \begin{cases} \dfrac{K}{1 + A \cdot \sigma_n^2(i,j)} & |D_n(i,j) - Z_n(i,j)| > T \\ 0 \quad otherwise \end{cases} \tag{7}$$

$$Z_n(i,j) = \begin{cases} D_{n-1}(i,j) & |D_{n-1}(i,j) - Z_{n-1}(i,j)| > T \\ Z_{n-1}(i,j) \quad otherwise \end{cases} \tag{8}$$

where $Z_n(i,j)$ is used to detect the temporal motion of each pixel, T is the threshold, and $\sigma_n^2(i,j)$ is the local spatial variance. The parameter K is the maximum step size. A is the normalization value. When the scene stays stillness, the value of learning rate is 0, which means the update of the NUC parameters is also paused. In this way the corrected image could be free from ghosting artifacts due to scene movement.

According to the whole process of LMS based algorithms, we can find that there are two key points which determine the quality of the NUC result, one is the accurate estimation of the desired image, and the other is the design of adaptive learning rate. The former determines the correct result whether closes to the ideal image, and the latter determines the convergence speed of NUC and accumulation of residuals which has great effect on ghosting artifact.

III. DESIRED IMAGE ESTIMATION BASED ON CO-OCCURRENCE FILTER

According to the analysis in section II, it's obvious that the estimation of desired image is crucial because an accurate desired image can keep the iteration process reducing the error in the right direction as well as eliminating the FPN. For the traditional neural network based NUC, the desired image is adopted by the mean value of the four neighbor pixels. Though the mean filter can smooth the FPN, it will also cause gradient distortion in detail and edge areas because the filter weight is always the same in the whole image. Besides, as the detail and edge are smoothed, the inappropriate correction coefficients in these areas will finally cause the ghosting artifact on the corrected image. Therefore, it's important to improve the filter that can distinguish the FPN and image details.

In order to reduce the FPN while reserve the image details, especially those areas with strong edges, this paper adopts a new kind of edge-preserve filter called co-occurrence filter to estimate the desired image. Co-occurrence filter (CoF) [20] is a novel boundary detection and edge preserving filters which can smooth noise within a textured region but not across texture boundaries. As shown in Fig.2, compared with other three filters, it can be seen that Fig.2(b) of GF result is so

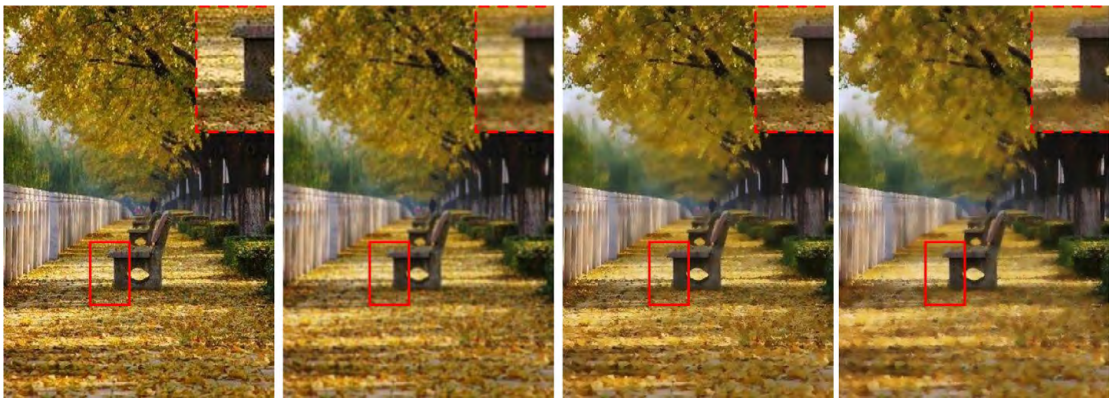

FIGURE 2. Comparison of the three filters' result. (a) Source image. (b) GF result. (c) BF result. (d) CoF result.

smooth that the image looks blurred. Fig.2(c) of BF result maintains the clarity of the whole image, but the smoothing effect is a little poor. However, in Fig.2(d), the edges of stone bench are preserved well and the textures between leaves are smoothed appropriately. It can be demonstratethat CoF result not only has a good smoothing effect but also preserves edges well.

The co-occurrence filter is derived from linear filters which is defined as following:

$$J_p = \frac{\sum_{q\in N(p)} w(p,q)\cdot I_q}{\sum_{q\in N(p)} w(p,q)} \tag{9}$$

where J_p and I_q are output and input pixel values, p and q are pixel indices, and $w(p, q)$ is the weight of the contribution of pixel q to the output of pixel p. In Gaussian filter, $w(p, q)$ is defined as following:

$$w(p,q) = \exp\left(-\frac{d(p,q)^2}{2\sigma_s^2}\right) \triangleq G_{\sigma_s}(p,q) \tag{10}$$

where $d(p, q)$ is the Euclidean distance in the image plane between pixel p and q, σ_s is the distributed parameter, $G_{\sigma_s}(p, q)$ means Gaussian filter. The CoF improves Gaussian filter with a normalized co-occurrence matrix to deal with boundaries. The expression is denoted as follows:

$$w(p,q) = G_{\sigma_s}(p,q)\cdot M(I_p, I_q) \tag{11}$$

$$M(a,b) = \frac{C(a,b)}{h(a)h(b)} \tag{12}$$

where M is a 256×256 matrix (in the case of the usual gray scale images) and calculated through co-occurrence matrix $C(a, b)$ which is counting the co-occurrence of values a and b divided by their frequencies. $h(a)$ and $h(b)$ are corresponding frequency with a and b in the image. Formally:

$$C(a,b) = \sum_{p,q} \exp\left(-\frac{d(p,q)^2}{2\sigma_c^2}\right)\left[I_p = a\right]\left[I_q = b\right] \tag{13}$$

$$h(k) = \sum_{p}\left[I_p = k\right] \tag{14}$$

where σ_c is a parameter of the co-occurrence matrix, when the value of σ_c goes to 0, CoF becomes a delta function that does not change the input image at all; When σ_c goes to ∞, CoF becomes the Gaussian filter. The value of $[\cdot]$ equals 1 when the inside expression is true, otherwise the value is 0. Finally, according to NUC model, the CoF function can be written as follows:

$$D = CoF(\sigma_s, \sigma_c, X) \tag{15}$$

where σ_s is set to 3, σ_c is usually set to $\sqrt{15}$. The CoF collects co-occurrence information directly from the image so that there is no need to adjust parameter when the CoF is applied to estimate the desired image for NUC of IRFPA. In theory, co-occurrence information collection should sample all pixel pairs in the image plane. In practice, we consider only pixel pairs within a window to enhance computational efficiency, the window size is usually set to 7.

IV. IMPROVED ADAPTIVE LEARNING RATE

The learning rate is another important factor to achieve good correction results. As mentioned above, the learning rate also determines the accumulation of residuals which has great effect on ghosting artifact. Commonly, residuals depend on the spatial geometric and are always sensitive to the edge or the boundary areas of image, which means a prerequisite of deghosting technique is that only pixels in the uniform region can be taken into account of update [21]. However, Hardie's algorithm [18] mainly considers temporal motion and gates the learning rate where the identical pixel in frame-by-frame is regarded as moving, therefore the edge areas or boundary textures of image will also be smoothed when the NUC parameters update according to the motion detection in Eq. (7) and (8). The residuals will slowly burn into the NUC parameters in these areas and finally the ghosting artifact generates. Moreover, the per-pixel temporal motion detection may also result in insufficient correction of FPN. For example, when a small bright target slides through a still scene during the image sequences, the NUC parameters only update the areas where target passed. As a result,

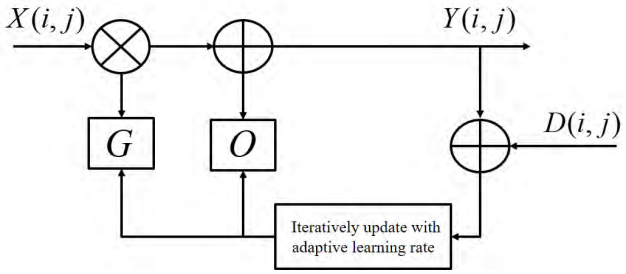

FIGURE 3. Flow chart of the proposed method of NUC.

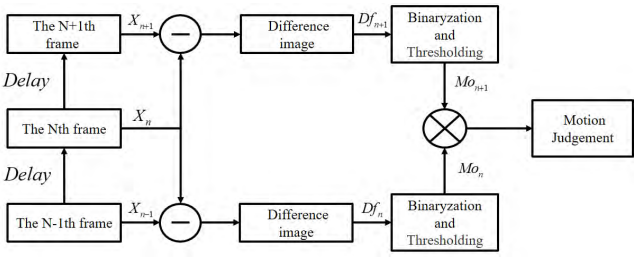

FIGURE 4. Block scheme of the motion guidance.

the FPN is eliminated only in local motion areas, and will be reserved in the background.

In order to solve the above problems and achieve a higher performance, an adaptive learning rate based on motion guidance and local spatial correlation detection is put forward to suppress the ghost effect, and the flow chart of the proposed method is showed in Fig.3. First the scene motion guidance is performed based on the improved three-frame difference method [22] which has better robustness compared to traditional temporal difference. All the NUC parameters will update if the current scene is estimated as moving, otherwise the parameters in the whole image remain unchanged. In this way the problem that insufficient correction of FPN could be solved. Moreover, as mentioned above, only consider temporal motion and gate the learning rate will cause the residuals because the NUC parameters in edge and boundary areas are not accurate, therefore we also use the local spatial correlation parameter [21] to find out the edge and boundary pixels of the image. The correction parameters corresponding to these pixels will remain the same during the NUC process and in this way the ghost artifact could be suppressed effectively.

Specifically, first we take three consecutive frames of image sequences as one observation period, and calculate the difference image of adjacent frames, that is:

$$Df_n(i,j) = |X_n(i,j) - X_{n-1}(i,j)| \tag{16}$$

where $Df_n(i,j)$ is the difference image, $X_n(i,j)$ is the output of IRFPA. Then the difference image is thresholding segmented and binarized which could be expressed as follows:

$$B_n(i,j) = \begin{cases} 255, & Df_n(i,j) > Th1 \\ 0, & Df_n(i,j) \le Th1 \end{cases} \tag{17}$$

where $B_n(i,j)$ is the binary image, $Th1$ is the segmentation threshold, the value of $Th1$ is usually set to 15.

For binary image $B_n(i,j)$, the median filter is used to eliminate the isolate noise in the image and then the number of pixels that value are equal to 255 is calculated. If the number exceeds threshold, the motion flag value corresponding to the current frame is set to 1, otherwise this value is set to 0, that is:

$$Mo_n = \begin{cases} 1, & N > Th2 \\ 0, & N \le Th2 \end{cases} \tag{18}$$

where Mo_n is the motion flag at the nth frame, N is the calculated number, $Th2$ is the statistical threshold and is usually set to 10.

For one observation period, each frame is calculated as Eq. (16)-(18) and the corresponding motion flag is acquired. Only all the value of motion flag equal to 1 and the scene is estimated as moving, and the NUC parameters will update, otherwise the parameters remain the same during the observation period. In summary, the process of motion guidance based on the improved three-frame difference method is indicated in Fig.4.

Then we use the local spatial correlation parameter to determine whether the detected pixel is belonging to edge or uniform region. It's defined as:

$$S_n(i,j) = \begin{cases} 1 & \forall (p,q) \in \Omega_r,\ |D_n(p,q) - D_n(i,j)| \le T_s \\ 0 & otherwise \end{cases} \tag{19}$$

where $S_n(i,j)$ is the local spatial correlation corresponding to the pixel (i,j), $D_n(i,j)$ is the desired image of NUC. Ω_r is the local search region around (i,j), the window size r is usually set to 5. (p,q) is the adjacent pixels included in Ω_r, T_s is a constant threshold of the local spatial correlation, and is set to 15.

Generally, when the local spatial correlation value of pixel (i,j) equals to 1, that means this pixel has high correlation with adjacent pixels, this pixel may be considered as uniform texture or background. However, when the value of local spatial correlation equals to 0, that means this pixel is quite different from the nearby regions, therefore this pixel is considered as edge or boundary texture.

Considering the idea of motion guidance and local spatial correlation detection, we can revise and gate the learning rate of NUC both in temporal and spatial domain. Combining Eq. (7), (18) and (19), the improved learning rate of NUC is defined as:

$$\lambda_n(i,j) = \begin{cases} \dfrac{K}{1 + A\sigma_n^2(i,j)} & S_n(i,j) \cdot Mo_n(i,j) \cdot Mo_{n+1}(i,j) = 1 \\ 0 & otherwise \end{cases} \tag{20}$$

The parameters K and A in Eq. (20) are the same as Eq. (7). The difference is that both the temporal motion detection and spatial correlation detection is used to gated

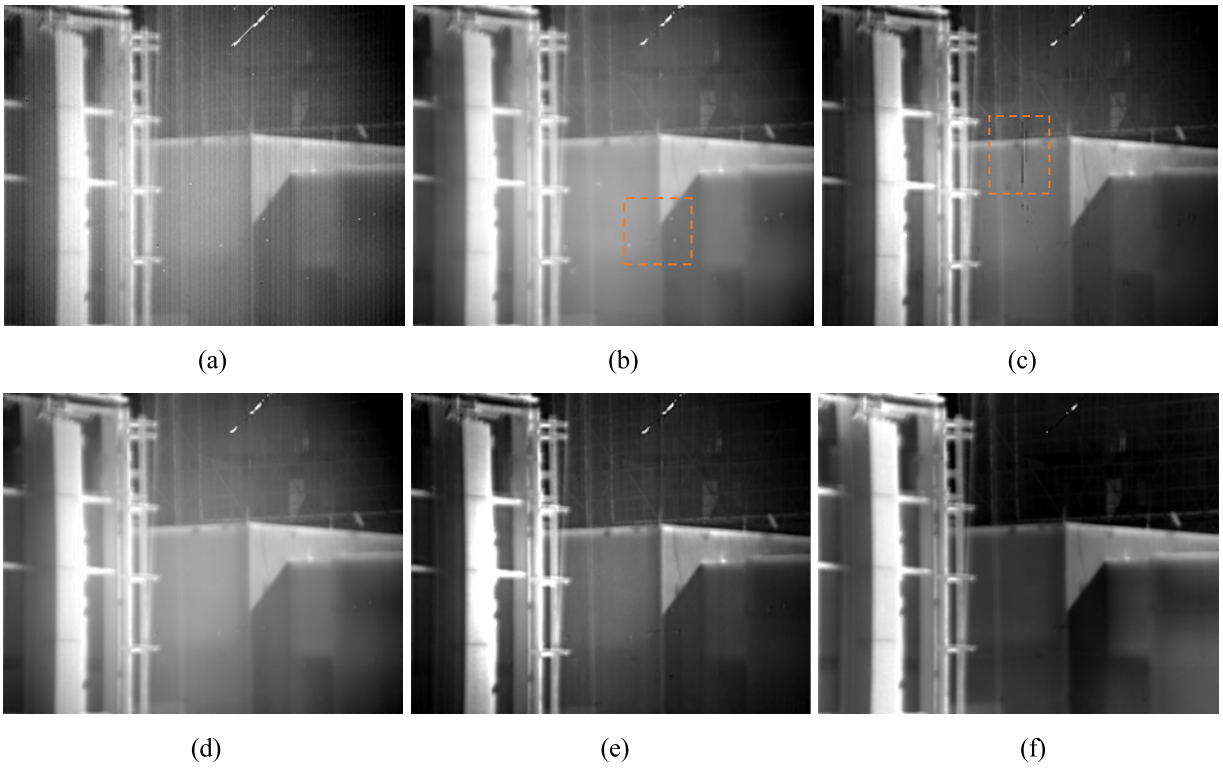

FIGURE 5. NUC results comparison of frame 120 of the first test sequence. (a) Uncorrected image. (b) Corrected with NN-NUC. (c) Corrected with BF-NUC. (d) Corrected with TV-NUC. (e) Corrected with GF-NUC. (f) Our methods.

the improved adaptive learning rate. Only if the current scene is moving and the detected pixel is located in uniform regions or background, the corresponding parameters of NUC can be updated. Therefore, the edge areas or boundary textures of image will be reserved all the time and the NUC parameters are always updated or retained simultaneously in the whole image, which is benefit to better visual effect of the image.

V. EXPERIMENTAL RESULTS

In this section, the infrared sequences with real non-uniformity are used to verify the performance and the robustness of the proposed method and other developed techniques. The infrared sequences are obtained from a long wave cooled IRFPA camera. Its resolution is 320 × 256, and the Analog/Digital sample precision is 14-bit. Detail information of this camera could be found in http://www.dali-tech.com/. The acquired sequences including the raw data without calibration correction in normal temperature and the data collected with two-point calibration in the IR window heating experiment. In this way the applicability and robustness of NUC methods could be verified.

Then, our NUC method is compared with NN-NUC method [13], BF-NUC method [14], GF-NUC method [17] and TV-NUC method [16]. In the proposed algorithm, the CoF distributed parameter σ_s is set to 3, co-occurrence matrix parameter σ_c is set to $\sqrt{15}$. Segmentation threshold $Th1$ and $Th2$ are set 15 and 10, individually. The window size of local spatial correlation r is 5 and constant threshold of the local spatial correlation T_s is set to 15. Finally, the maximum step size K is 1e-3 and normalization value A is 1.

Fig.5-7 shows the different correction results in a frame of Media1-Media3. (a) are original non-uniformity images, (b) are the results of NN-NUC, (c) are the results of BF-NUC, (d) are the results of Vera's TV-NUC, (e) are the results of GF-NUC and (f) are the results of proposed method, respectively. Media1 and Media2 are collected in the outdoor environment with normal temperature, and Media3 is collected in the laboratory with a heated IR window placed in front of the lens to simulate the aero-heating effect.

Fig.5 and Fig.6 are the outdoor scenes which include buildings, fence, sky and cloud. It can be seen that the stripe FPN influenced the original image quality seriously, and there are also some fix and random blind pixels appear during the image acquisition, which reduce the image quality even further. According to the comparing results, it's obvious that the proposed method visually performed much better than other four methods. For NN-NUC and BF-NUC methods, the results are smoothed a lot and some edge and detail information in the scenes are missing, such as the scaffold of buildings, wire of the fence in Fig.6(b) and (c). Moreover, the results also produce visible ghosting artifacts or diffusion spot in the area where the random blind pixels appear in Fig.5(b) and (c). For TV-NUC and GF-NUC methods, a little uniformity is still remained, and some edge or details in the image are also over smoothed. However, the proposed

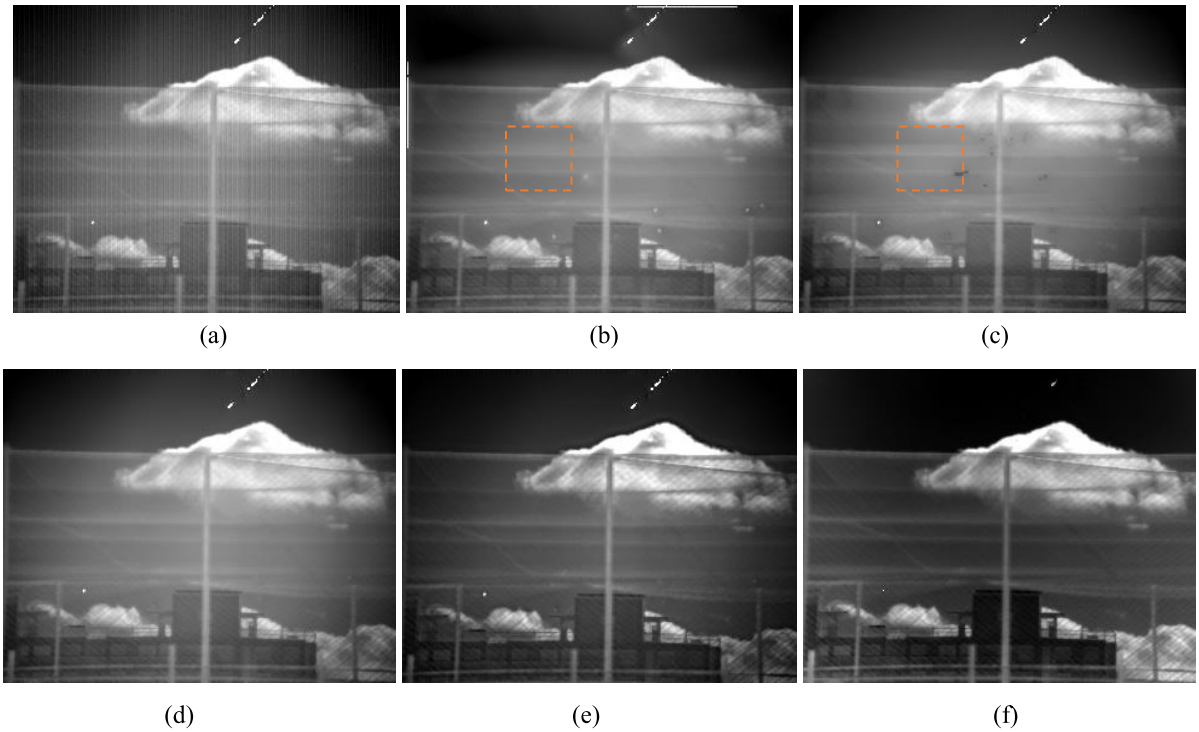

FIGURE 6. NUC results comparison of frame 100 of the second test sequence. (a) Uncorrected image. (b) Corrected with NN-NUC. (c) Corrected with BF-NUC. (d) Corrected with TV-NUC. (e) Corrected with GF-NUC. (f) Our methods.

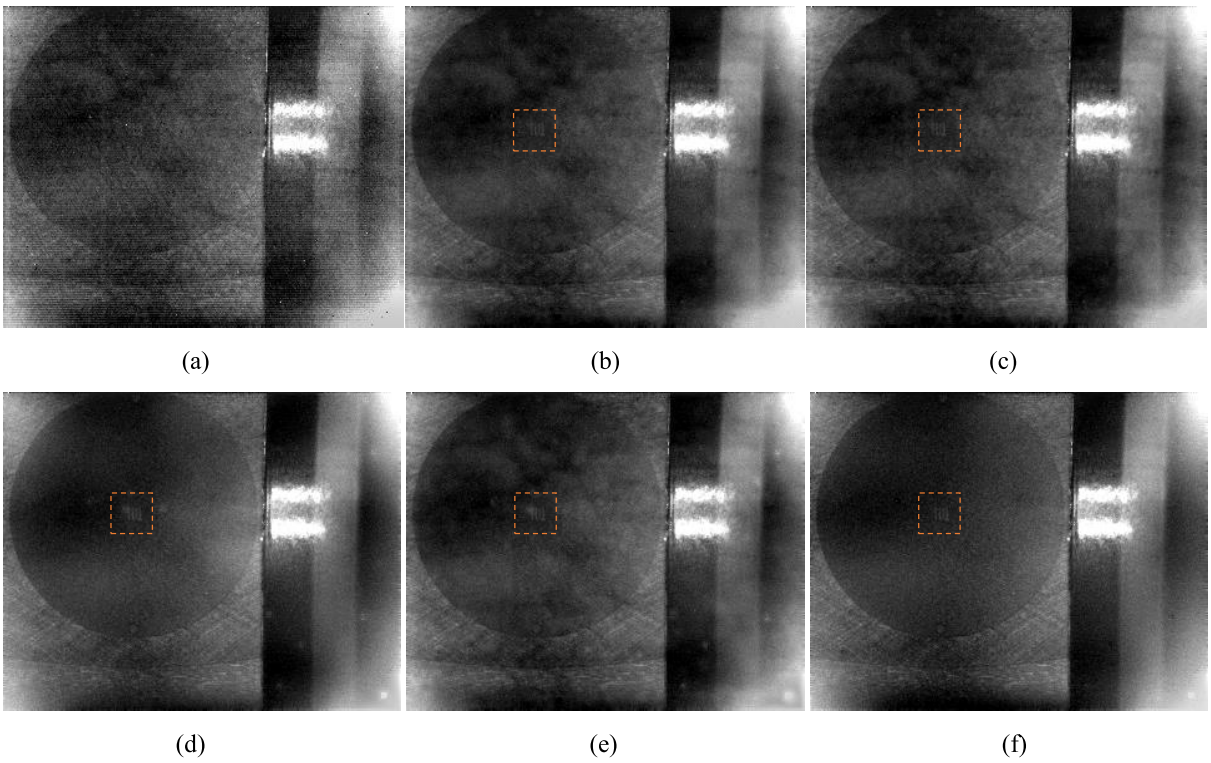

FIGURE 7. NUC results comparison of frame 150 of the target test sequence. (a) Uncorrected image. (b) Corrected with NN-NUC. (c) Corrected with BF-NUC. (d) Corrected with TV-NUC. (e) Corrected with GF-NUC. (f) Our methods.

method provides good balance between NUC and details preservation. In Fig.5(f) and Fig.6(f), stripe FPN is almost removed completely and the ghosting artifact scarcely exists in the scene, which means the results of the proposed NUC method has better visual effect and subjective view.

TABLE 1. Comparison of roughness index ρ for Figs. 5-7.

	frame	Original	NN-NUC	BF-NUC	TV-NUC	GF-NUC	Proposed
Media 1	120th	0.198	0.159	0.165	0.149	0.142	0.131
Media 2	100th	0.096	0.082	0.079	0.077	0.076	0.072
Media 3	150th	0.192	0.143	0.141	0.133	0.138	0.116

TABLE 2. Comparison of average processing time for three media data (unit: millisecond/ms).

	Image size	NN-NUC	BF-NUC	TV-NUC	GF-NUC	Proposed
Media 1	320×256	5.627	18.431	9.035	21.824	12.795
Media 2	320×256	5.462	19.658	8.769	23.248	11.582
Media 3	320×256	4.973	19.216	9.855	22.714	13.147

Fig.7 shows the 150th frame of Media 3 which is collected in the IR window heating experiment to simulate the aero-heating effect on IR imaging system. Fig. 7(a) is the original target test image as window temperature is up to 673K, it's obvious that there exists much stripe FPN and non-uniformity noise. Fig.7(b)-(e) are other NUC methods, as shown above, the FPN and non-uniformity noise still remained in the images, and the target in the center cannot be distinguished. The proposed method performances much better than other methods and the NUC result is shown in Fig. 7(f). It can be seen that most non-uniformity noise is eliminated and the target in the center is clear and distinct, which means this method can significantly improve the resolution and minimum resolvable temperature difference(MRTD) of infrared imaging systems.

VI. DISCUSSION

To make quantitative and objective evaluation of NUC algorithm performance, we introduce a reference-free roughness index ρ which measures the high-pass content of the input image [14], [17]. And it's also used for evaluating the performance of NUC. It's defined as:

$$\rho = \frac{\|h_1 * I(i,j)\|_1 + \|h_2 * I(i,j)\|_1}{\|I(i,j)\|_1} \tag{21}$$

where $h_1 = [1, -1]$ and $h_2 = h_1^T$ are horizontal and vertical mask for image, the asterisk denotes discrete convolution, and $||\_||_1$ denotes L1 norm; $I\ (i, j)$ is gray intensity. Smaller value of ρ is expected in NUC image process.

Then we carried out experiments for investigated NUC methods by visual studio 2013 on a personal computer using Windows (2.3GHz Intel Core 2 CPU, 8GB memory).

According to the experiment and evaluated results, we further analyze the performance of the proposed algorithm in two aspects:

A. APPLICABILITY AND ROBUSTNESS

The evaluated results of roughness index ρ for Fig.5-7 are listed in TABLE 1. According to the evaluation, the proposed method always performed better than any other NUC algorithms which failed in details preservation or ghosting artifacts suppression. For example, the result of NN-NUC and BF-NUC methods in Fig.5(b) and Fig.5(c), there exist visible ghosting artifacts, and for the result of TV-NUC and GF-NUC methods in Fig.6(d) and Fig.6(e), the details of the fence are lost. However, the proposed one removed the non-uniformity as well as preserved details with less ghosting artifacts simultaneously. Besides, as for bad imaging conditions in Media3, the result of the proposed one is also much better than others, most non-uniformity noise and stripe FPN are removed and the target is visible. All the results prove that the proposed method performs best, working robustly and excellently in different environment.

B. COMPUTATIONAL COST AND EFFICIENCY

Speed and efficiency is another important metric for NUC method evaluation. In order to compare the efficiency of NUC methods, we calculate the processing time of the five methods, and the result is listed in TABLE 2.

According to TABLE 2, NN-NUC runs fastest, and GF-NUC runs slowest. The efficiency of proposed method is higher than BF-NUC and GF-NUC, but works not as fast as the simple model based algorithms. Luckily, all the method can achieve the real-time processing on the work computer. Therefore, it's possible to further improve efficiency and reduce the computational cost for the better application in real-time IR system.

The convergence speed is also an important metric for algorithm efficiency. The results of Media 1-3 are listed in Fig.8. In Fig.8(a) and (b), since the scene varies all the time, most areas of the image can get enough movement. Due to the edge-preserve filter we used, the proposed method has better performance of removing non-uniformity and it has smaller value of roughness. In Fig. 8(c), the scene is static during the first 30 frames, and then the scene is moving and NUC methods start to work. Compared with other methods, the proposed one has a steeper descent gradient and the roughness value is also much better than others. Therefore, we can conclude that the proposed method performed better in convergence speed.

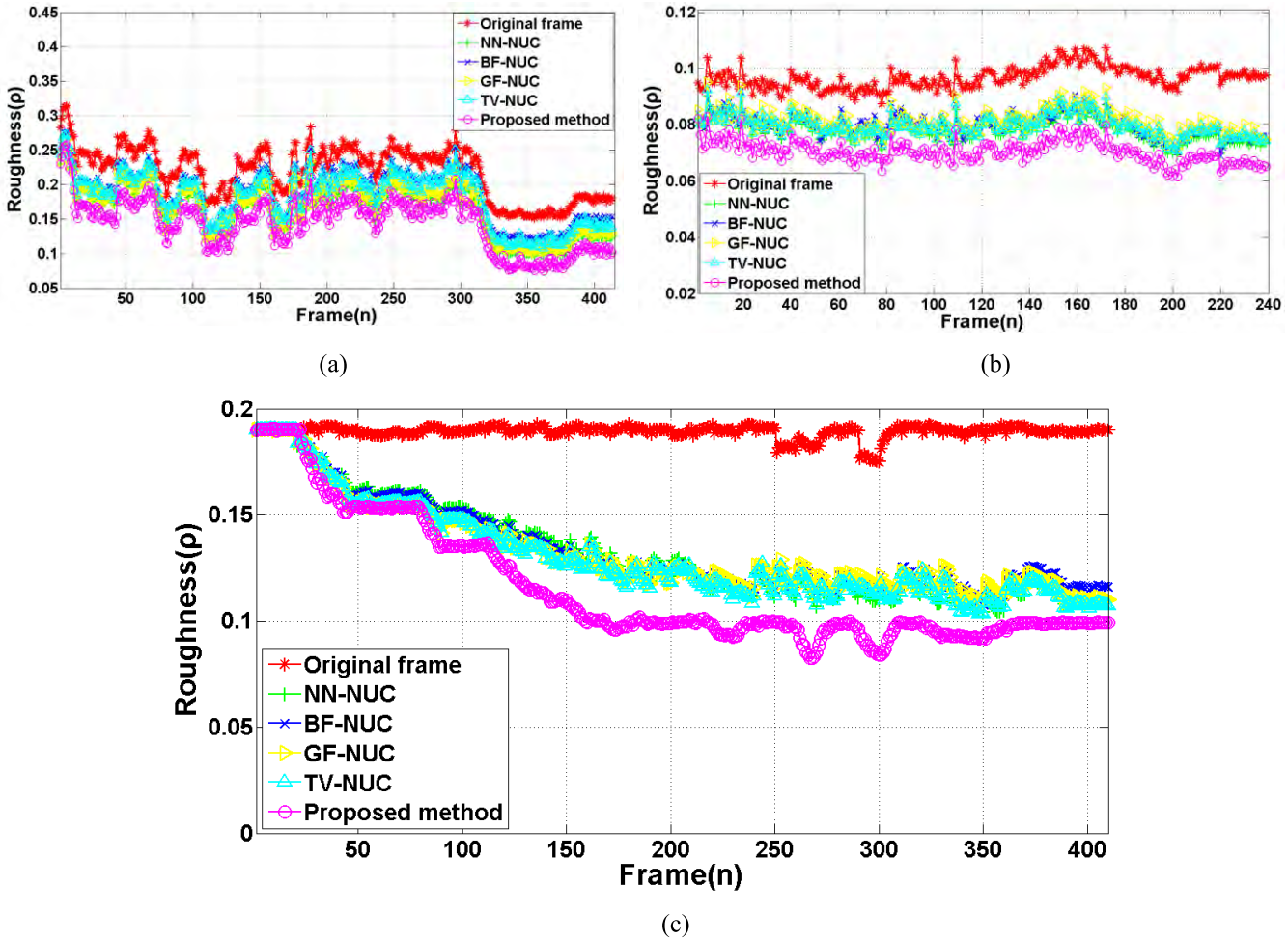

FIGURE 8. Comparison the convergence speed of roughness of the three test sequences. (a) Roughness of the first test sequence. (b) Roughness of the second test sequence. (c) Roughness of the third test sequence.

In summary, all the experiment results above indicate that the proposed algorithm excellently balances the correction result and the visual effect, and has better performance of in the aspects of applicability and robustness.

VII. CONCLUSION

In this paper, a novel scene-based non-uniformity correction method of IRFPA was proposed. By using the co-occurrence filter and the adaptive learning rate connected with both temporal motion and spatial correlation factor, this algorithm can effectively eliminate the fixed pattern noise as well as suppress the potential ghost artifact in the image. Experiments with several infrared sequences demonstrate that the performance of the proposed method is better than other classic algorithms. The correction result has fewer noise and scarcely exists ghosting artifact, which is suitable for the application in practical infrared image system. Considering the real-time requirement in application, the enhancement of computational efficiency and the convergence speed should be studied deeper in the future work, and our method could be also considered applying to other image processing fields.

REFERENCES

[1] D. A. Scribner, M. R. Kruer, and J. M. Killiany, "Infrared focal plane array technology," *Proc. IEEE*, vol. 79, no. 1, pp. 66–85, Jan. 1991.
[2] O. Riou, S. Berrebi, and P. Bremond, "Nonuniformity correction and thermal drift compensation of thermal infrared camera," *Proc. SPIE*, vol. 5405, pp. 294–302, Apr. 2004.
[3] T. Orżanowski and H. Madura, "Test and evaluation of reference-based nonuniformity correction methods for microbolometer infrared detectors," *Opto-Electron. Rev.*, vol. 18, no. 1, pp. 91–94, Mar. 2010.
[4] J. Zhao *et al.*, "Single image stripe nonuniformity correction with gradient-constrained optimization model for infrared focal plane arrays," *Opt. Commun.*, vol. 296, pp. 47–52, Jun. 2013.
[5] J. G. Harris and Y.-M. Chiang, "Nonuniformity correction of infrared image sequences using the constant-statistics constraint," *IEEE Trans. Image Process.*, vol. 8, no. 8, pp. 1148–1151, Aug. 1999.
[6] D. A. Scribner *et al.*, "Adaptive retina-like preprocessing for imaging detector arrays," in *Proc. IEEE Int. Conf. Neural Netw.*, Mar./Apr. 1993, vol. 3823, no. 7, pp. 1955–1960.
[7] W. Qian, Q. Chen, and G. Gu, "Space low-pass and temporal high-pass nonuniformity correction algorithm," *Opt. Rev.*, vol. 17, no. 1, pp. 24–29, Jan. 2010.
[8] C. Zuo, Q. Chen, W. Qian, and G. Gu, "New temporal high-pass filter nonuniformity correction based on bilateral filter," *Opt. Rev.*, vol. 18, no. 2, pp. 197–202, Mar. 2011.
[9] Z. Li, T. Shen, and S. Lou, "Scene-based nonuniformity correction based on bilateral filter with reduced ghosting," *Infr. Phys. Technol.*, vol. 77, pp. 360–365, Jul. 2016.

[10] C. Zuo, Q. Chen, X. Sui, and G. Gu, "Scene-based nonuniformity correction algorithm based on interframe registration," *J. Opt. Soc. Amer. A, Opt. Image Sci.*, vol. 28, no. 6, pp. 1164–1176, Jun. 2011.
[11] C. Zuo, Q. Chen, G. Gu, X. Sui, and J. Ren, "Improved interframe registration based nonuniformity correction for focal plane arrays," *Infr. Phys. Technol.*, vol. 55, no. 4, pp. 263–269, 2012.
[12] J. Zhao, X. Gao, Y. Chen, H. Feng, Z. Xu, and Q. Li, "Fast iterative adaptive nonuniformity correction with gradient minimization for infrared focal plane arrays," *Infr. Phys. Technol.*, vol. 65, pp. 87–93, Jul. 2014.
[13] D. A. Scribner, K. A. Sarkady, M. R. Kruer, J. T. Caulfield, J. D. Hunt, and C. Herman, "Adaptive nonuniformity correction for IR focal-plane arrays using neural networks," *Int. Soc. Opt. Photon.*, vol. 1541, pp. 100–110, Nov. 1991.
[14] A. Rossi, M. Diani, and G. Corsini, "Bilateral filter-based adaptive nonuniformity correction for infrared focal-plane array systems," *Opt. Eng.*, vol. 49, no. 5, May 2010, Art. no. 057003.
[15] E. Vera, P. Meza, and S. Torres, "Total variation approach for adaptive nonuniformity correction in focal-plane arrays," *Opt. Lett.*, vol. 36, no. 2, pp. 172–174, 2011.
[16] E. Vera, P. Meza, and S. Torres, "Total variation adaptive scene-based nonuniformity correction," *Opt. Soc. Amer.*, vol. 27, no. 5, Jun. 2010, Art. no. JTuA24.
[17] R. Sheng-Hui, Z. Hui-Xin, Q. Han-Lin, L. Rui, and Q. Kun, "Guided filter and adaptive learning rate based non-uniformity correction algorithm for infrared focal plane array," *Infr. Phys. Technol.*, vol. 76, pp. 691–697, May 2016.
[18] R. C. Hardie, F. Baxley, B. Brys, and P. Hytla, "Scene-based nonuniformity correction with reduced ghosting using a gated LMS algorithm," *Opt. Express*, vol. 17, no. 17, pp. 14918–14933, Aug. 2009.
[19] Y. Chang, H. Fang, L. Yan, and H. Liu, "Robust destriping method with unidirectional total variation and framelet regularization," *Opt. Express*, vol. 21, no. 20, pp. 23307–23323, Oct. 2013.
[20] R. J. Jevnisek and S. Avidan, "Co-occurrence filter," in *Proc. IEEE Conf. Comput. Vis. Pattern Recognit.*, Jul. 2017, vol. 406, no. 10, pp. 3184–3192.
[21] F. Fan, Y. Ma, J. Huang, Z. Liu, and C. Liu, "A combined temporal and spatial deghosting technique in scene based nonuniformity correction," *Infr. Phys. Technol.*, vol. 71, pp. 408–415, Jul. 2015.
[22] X. Han, Y. Gao, Z. Lu, Z. Zhang, and D. Niu, "Research on moving object detection algorithm based on improved three frame difference method and optical flow," in *Proc. 5th Int. Conf. Instrum. Meas., Comput., Commun. Control*, vol. 283, no. 19, Sep. 2015, pp. 580–584.

LI LINGXIAO received the B.E. degree in optic and electrical engineering from Chongqing University, in 2014. He is currently pursuing the Ph.D. degree in optic engineering with Zhejiang University. He has participated in the completion of two military exploration projects and authored several journal/conference papers and patents. His research interests include new optical imaging technology, image processing algorithm, and its applications in real image systems.

LI QI received the Ph.D. degree in optical engineering from Zhejiang University, in 2004. As the project leader, he has undertaken a number of national, provincial, and ministerial research projects, and received twice second prizes from Zhejiang Science and Technology. He published more than 30 SCI papers in *Optics Letters*, *Applied Optics*, *Optics & Laser Technology*, *Optical Engineering*, and *Optics & Laser in Engineering*. In recent years, he has applied for more than 20 invention patents. His current research interests include optical engineering, imaging technology, image acquisition, and processing.

FENG HUAJUN was promoted as a Professor and a Ph.D. Supervisor, in 1998. He was the Director of the Department of Optoelectronics, Zhejiang University, and the Director of the Institute of Optical Engineering. He is currently the Director of the Institute of Optical Imaging Engineering, Zhejiang University. He has been responsible for several key projects of the National Natural Science Foundation, the State Education Commission, the Ministry of Science and Technology, the 973 and 863 Projects, and the Lunar Exploration Project. He authored more than 40 invention patents and published more than 100 academic papers in the past five years, including more than 100 papers by SCI, EI, and ISTP.

XU ZHIHAI received the Ph.D. degree in optical engineering from Zhejiang University, in 1996. He studied and was a Visiting Scholar with the State University of New Jersey and the University of Illinois at Urbana–Champaign. He was the Deputy Director of the Optoelectronics Department, Zhejiang University Information Institute, and the Secretary General of the Zhejiang Optical Society. In the past ten years, as the Project Leader, he has undertaken many scientific research projects. As the first completion person, he received the first prize of National Defense Technology Invention and the second prize of Science and Technology of Zhejiang Province. He has published three academic monographs, published more than 120 papers in SCI/EI, and holds more than 60 national patents. He received the Outstanding Contribution Award by the National Science and Technology Plan of the Eleventh Five-Year Plan and also received the title of Young and Middle-aged Expert with Outstanding Contribution in Zhejiang Province.

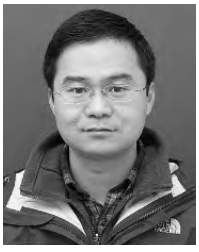

CHEN YUETING received the Ph.D. degree in optical engineering from Zhejiang University, in 2009. He has undertaken several national, provincial and ministerial research projects, and published more than 30 SCI/EI papers. Besides, he has applied for more than 20 invention patents. His current research interests include optical engineering, imaging technology, computer vision, and processing.